Mössbauer spectroscopy evidence of intrinsic non-stoichiometry in iron telluride single crystals

Airat G. Kiiamov[1,2], Yury V. Lysogorskiy[1], Farit G. Vagizov[1], Lenar R. Tagirov[1,3], Dmitrii A. Tayurskii[1,2], Dorina Croitori[4], Vladimir Tsurkan[4,5,], and Alois Loidl[5]*

The FeTe parent compound for iron-superconductor chalcogenides was studied applying Mössbauer spectroscopy accompanied by *ab initio* calculations of electric field gradients at the iron nuclei. Room-temperature (RT) Mössbauer spectra of single crystals have shown asymmetric doublet structure commonly ascribed to contributions of over-stoichiometric iron or impurity phases. Low-temperature Mössbauer spectra of the magnetically ordered compound could be well described by four hyperfine-split sextets, although no other foreign phases different from $Fe_{1.05}Te$ were detected by XRD and microanalysis within the sensitivity limits of the equipment. Density functional *ab initio* calculations have shown that over-stoichiometric iron atoms significantly affect electron charge and spin density up to the second coordination sphere of the iron sub-lattice, and, as a result, four non-equivalent groups of iron atoms are formed by their local environment. The resulting four-group model consistently describes the angular dependence of the single crystals Mössbauer spectra as well as intensity asymmetry of the doublet absorption lines in powdered samples at RT. We suppose that our approach could be extended to the entire class of $Fe_{1+y}Se_{1-x}Te_x$ compounds, which contain excess iron atoms.

1 Introduction

Discovery of superconductivity with a critical temperature of 26 K in fluorine-doped LaFeAsO has triggered worldwide search of iron-based superconductors since 2008 [1]. These efforts have brought up a family of superconducting iron compounds which show critical temperatures up to 55 K [2]. Five different structural classes of iron-based superconductors have been identified. All of them share a common structure based on a planar layer of iron atoms, joined by tetrahedrally coordinated pnictogen (P, As) or chalcogen (S, Se, Te) anions, arranged in a stacked sequence separated by alkali, alkaline-earth or rare-earth metals and oxygen/fluorine blocking layers [2–4]. Tetragonal FeSe is the simplest compound with similar structure, which shows superconductivity below a critical temperature of 8 K [5]. Moreover, external pressure dramatically raises the critical temperature up to 27 K [6] and even more [7]. Thus, the next step was to apply internal pressure by chemical modification of the original compound.

In Ref. [8] it was shown that Te-doping of FeSe can increase the critical temperature up to 14 K. At room temperature, FeSe, FeTe, and $Fe(Se_{1-x}Te_x)$ systems have similar layered lattice structure that simplifies Te-doping of the FeSe compound [5, 9]. Nevertheless, it is well known that FeTe always grows with excess iron atoms [9–11] which affect the electronic properties [12] and complicate magnetic order [13, 14] of the $Fe_{1+y}Te$ compound. Inevitably, excess iron will show up in $Fe_{1+y}(Se_{1-x}Te_x)$ systems (for $x > 0$) [9, 15–18]. In recent years, a number of theoretical investigations of $Fe_{1+y}(Se_{1-x}Te_x)$ systems [19–24]was published. It was predicted [12] that excess iron atoms in the $Fe_{1.125}Te$ compound are strongly magnetic, and their calculated magnetic moment is about 2.5 μ_B. On the other hand, in the FeSe compound

* Corresponding author: E-mail: vladimir.tsurkan@physik.uni-augsburg.de

[1] Institute of Physics, Kazan Federal University, 420008 Kazan, Russia

[2] Centre for Quantum Technologies, Kazan Federal University, 420008 Kazan, Russia

[3] E.K. Zavoisky Physical-Technical Institute, Russian Academy of Sciences, 420029 Kazan, Russia

[4] Institute of Applied Physics, Academy of Sciences of Moldova, MD-2028 Chisinau, R. Moldova

[5] Experimental Physics V, University of Augsburg, 86159 Augsburg, Germany

excess iron atoms dramatically influence or even destroy superconductivity [25]. One could argue, in general, that over-stoichiometric iron atoms significantly affect the physical properties of FeSe and, possibly, FeTe and $Fe(Se_{1-x}Te_x)$ compounds.

In the present paper we employ Mössbauer spectroscopy to study excess iron atoms in $Fe_{1.05}Te$. Observation of the fine structure of the Mössbauer spectra complemented by *ab initio* calculations of the electric field gradients (EFG) on iron nuclei allows establishing a statistical distribution of excess iron atoms over the FeTe lattice. We argue that unexpected asymmetry of Mössbauer spectra reported in numerous papers for powdered samples [26–29] can be attributed to over-stoichiometric iron atoms and their influence on the regular iron atoms in the $Fe_{1+y}(Se_{1-x}Te_x)$ type compounds.

The paper is organized as follows: first we provide the sample preparation and characterization data, then we describe Mössbauer experimental details, and present experimental results. Further, we give the basics of *ab initio* calculations used in the present work, and provide calculated data for the electric field gradients. Next, the analysis and comparison of the experimental and *ab initio* calculated parameters of the Mössbauer spectra are given. Finally, the conclusion section summarizes findings of the present study.

2 Crystal structure and sample preparation

FeTe is isostructural with α-PbO and crystallizes in tetragonal lattice (P4/nmm space group) which is analogous to a structure of superconducting FeSe [9]. In FeTe iron atoms can occupy two different crystallographic positions [10, 11]. Iron atoms in the first position (2a) form Fe-Te layers with tellurium atoms while iron atoms in the second position (2c) are located in the interlayer space between the Fe-Te layers. The 2a position is usually fully occupied [15, 30–32] while the occupancy "y" of the 2c position might be up to $y = 0.2$ [9, 15, 26]. In literature, iron atoms in these 2a and 2c positions are ordinarily marked as Fe1 and Fe2, respectively. We will use these notations further in the present work. The presence of Fe2 atoms leads to non-stoichiometry, $Fe_{1+y}Te$, so, this iron is considered as excess atom [12].

Single crystals of FeTe were grown by the Bridgman method. For the preparation, the elemental Fe of 99.99% purity was used. The elemental Te of purity 99.999% was additionally purified by zone melting to remove the oxide impurity. The starting materials in the stoichiometry $Fe_{1.1}Te$ were loaded into a double quartz ampoule, pumped to 10^{-2} mbar and closed. The ampoule was heated with a rate of 300 °C/h to 1100 °C, soaked for 5 h at this temperature and then slowly pulled with a rate of 3 mm/h through the temperature gradient of 350 °C. The final cooling rate was 60 °C/h to room temperature. The solidified ingot showed clear signs of phase separation, with a non-crystallized upper part and a shiny mirror-like single crystalline bottom part. The bottom part was easily cleaved and the samples from this part were used for the studies.

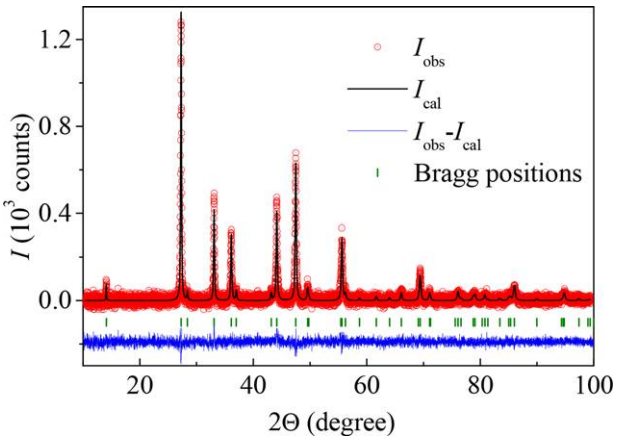

Figure 1 (color online) Rietveld refinement of the grounded single crystals of $Fe_{1+y}Te$. Red circles show the observed intensity, black solid line - the calculated pattern, blue line - the difference between the observed and calculated patterns, green vertical lines show the Bragg reflections.

The XRD studies of a grounded single crystals by conventional powder diffractometer (STADI-P, STOE&CIE) did not find any non-reacted impurities. The x-ray diffraction pattern together with the Rietveld refinement is shown in Fig 1. The Rietveld analysis of the XRD pattern was performed based on the tetragonal lattice of P4/nmm symmetry. The lattice constants $a = b = 3.8259(2)$ Å, $c = 6.2832(6)$ Å. The refined overall stoichiometry of Fe = Fe1 + Fe2 = 1.094 fits well the initially charged 1.1. At the same time, the refinement shows that the site occupation for the tetrahedral Fe1 is only 0.964, while the interstitial Fe2 site has the occupancy of 0.130. Single crystal x-ray diffraction analysis confirmed the crystallographic plane (001) to be the surface cleavage plane of the samples.

The composition of the sample was measured by wave-length-dispersive x-ray electron-probe microanalysis (WDS EPMA, Cameca SX50). The data were averaged over 10 points with surface of 70 × 60 μm^2 measured on different parts of the single crystalline sample. The obtained resulting composition is $Fe_{1.052(4)}Te$. In the brackets the standard deviations are given. We note

that the stoichiometry obtained by the WDS analysis deviates strongly from that determined by the Rietveld refinement. However, because the WDS analysis is an absolute method, we think that it gives more reliable results than the Rietveld analysis. The observed phase separation of the ingot also suggests the deviation of the composition of the grown crystal from the starting charge. However, one can not also fully exclude some inhomogeneity of the distribution of the Fe ions along the ingot.

3 Mössbauer spectroscopy

3.1 Mössbauer spectroscopy setup

Mössbauer-effect measurements were carried out in a temperature range from 4.2 K to 295 K (RT), using a conventional constant-acceleration spectrometer (WissEl, Germany) with ^{57}Co of about 40 mCi activity in a rhodium matrix as γ-radiation source.

Several types of a sample (absorber) were used: (a) a high quality single crystal of $Fe_{1.05}Te$ in plate form at room temperature (RT) and (b) a set of thin flakes, cut from the single-crystal ingot and packed with surface orientation parallel to the cleavage plane (001) for the measurements at low temperatures (LT). In addition, a powder sample of $Fe_{1.05}Te$ obtained by milling of single crystal ingots was measured at RT.

Orientation angle (β) between the crystallographic c-axis of the crystal (which is normal to the surface of the considered samples) and propagation direction of γ-photons (k-vector) was close to 0° for all temperatures, and to 47° for one control measurement at RT (see below).

Low-temperature measurements were carried out with a continuous flow cryostat (model CFICEV from ICE Oxford, UK). At RT a metallic-iron foil was used for velocity calibration of the Mössbauer spectrometer. Isomer shifts were referred to α-Fe at RT.

3.2 Experimental results

Room-temperature Mössbauer spectra of high quality single crystal sample were obtained in two velocity ranges: (i) in broad velocity range from −5.5 mm/s to 5.7 mm/s for confirmation of the absence of impurity phases, and (ii) in velocity range from −2 mm/s to 2 mm/s in order to obtain accurate line shape. They are displayed in Fig. 2. One observes an asymmetric quadrupole doublet. Such form of the spectrum indicates the paramagnetic state of iron atoms in the compound. The absence of magnetic order at RT was

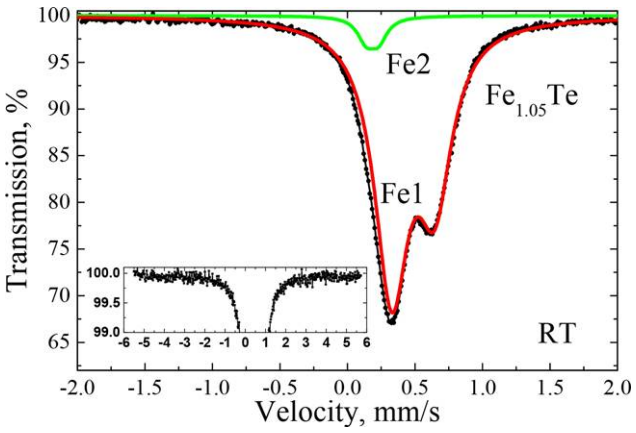

Figure 2 (color online) The room-temperature Möessbauer spectra of $Fe_{1.05}Te$ single-crystalline sample fitted by two doublets (see details in the body text). Inset - zoomed spectrum obtained in wide velocity range.

previously reported in Refs. [26, 33] for FeSe, $Fe_{1.08}Te$, and $Fe(Se_{0.5}Te_{0.5})$ systems. The Mössbauer spectrum obtained in the wide velocity range does not contain any other components that could correspond to traces of impurity phases being ferromagnetic at RT and having large hyperfine fields at iron iron nuclei (inset on Fig. 2). This fact also agrees with the results of the XRD phase analysis presented in Section 2.

As a first approximation the RT spectrum of $Fe_{1.05}Te$ can be described by two lines ascribed to iron atoms in different crystallographic positions. Such approach was already used in Ref [26]. The spectra were fitted implying that the doublet lines have Lorentzian shape with equal linewidth, and using the transmission integral [34]. Results of the fitting are depicted on Fig. 2 by thin solid lines. Weights of about 95% and 5% were obtained for Fe1 and Fe2 sub-spectra, respectively, which agree with the actual composition of $Fe_{1.05}Te$ obtained with WDS. The doublet corresponding to Fe2 (green line) shows a symmetric profile. The main doublet (red line) referred to Fe1 atoms exhibits a peak-amplitude ratio 3: 1.9. On the other hand, for the case of layered structure with axial symmetry, when the angle θ between k-vector of radiation and principal axis of EFG tensor is zero, the theoretically predicted peak-amplitude ratio for the single crystal should be 3: 1. The experimental deviation of the predicted asymmetry could be due to several reasons: (i) the c-axis is not perpendicular to the sample surface; (ii) presence of impurity phases; or (iii) influence of the Goldanski-Karyagin effect [35].

The perpendicular orientation of the crystalline c-axis with respect to the sample surface as well as the absence of impurity phases were proven by XRD and Mössbauer

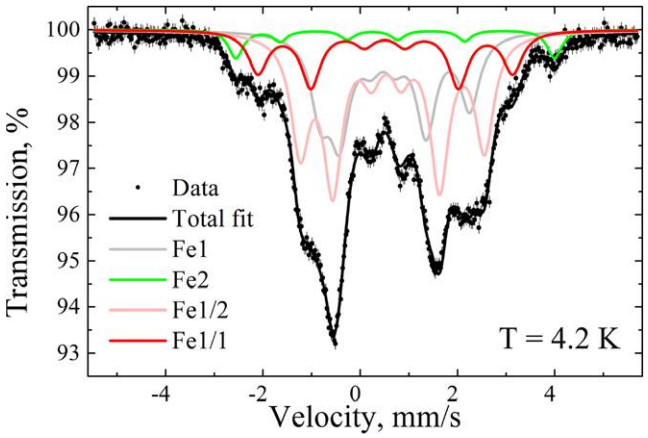

Figure 3 (color online) Mössbauer spectrum of $Fe_{1.05}Te$ single-crystalline sample obtained at 4.2 K and fitted by four sextets. Each sextet can be assigned to nonequivalent iron centers - Fe1, Fe2, Fe1/1, and Fe1/2, see Section 5 (Discussion).

spectroscopy measurements in wide velocity range. So, reasons (i) and (ii) could be excluded. The asymmetry of the doublet lines, related to Goldanski-Karyagin effect, should become weaker at low temperatures [35], whereas our Mössbauer spectrum at 80 K is still asymmetric with the intensity ratio for the Fe1 doublet of about the same 3: 1.9. Thus, we can assume that influence of Goldanski-Karyagin effect on the asymmetry of the doublet lines is negligible. Therefore, we conclude that the observed asymmetry of the Mössbauer spectra could be a result of some intrinsic property of the $Fe_{1.05}Te$ compound.

Figure 3 shows a Mössbauer spectrum at 4.2 K obtained with the sample, which was a set of thin flakes, cut from the single-crystal ingot and packed with surface orientation parallel to the cleavage plane (001). As can be seen it has a complex shape with a number of lines which could be attributed to several magnetic sextets. It is known that at low temperatures $Fe_{1+y}Te$ is antiferromagnetic [26] and has $P2_1/m$ space group symmetry, however, the number of crystallographic positions of iron atoms remains the same as for the RT structure [30]. The magnetic order at LT leads to splitting of the doublets into sextets in the Mössbauer spectrum. The minimal number of sextets which allows to describe accurately the LT spectrum (Fig. 3) was found equal to four. The fit to the LT spectrum is presented on Fig. 3 as black line, the hyperfine parameters of subspectra such as hyperfine field (*HS*), quadrupole splitting (*QS*), lines intensity (I_i) and partial area (*W*) are presented in Table 1. As can be seen from the Table 1, the quadrupole splitting to hyperfine field energy ratio $E_{QS}/E_{HF}<1$ that relaxes requirement of the full Hamiltonian analysis to

Table 1 The hyperfine parameters of the subspectra obtained as a result of LT Moessbauer spectrum fit (Fig. 3).

Sextet	HS, kOe	QS, mm/s	I_1, I_6	I_2, I_5	I_3, I_4	W
Gray	95.(2)	0.25	3.0	4.0	1.0	0.31
Green	202.(9)	0.46	3.0	1.2	1.0	0.05
Pink	117.(3)	0.12	3.0	4.0	1.0	0.46
Red	162.(3)	0.01	3.0	4.0	1.0	0.18

determine the hyperfine structure parameters within accuracies of our measurements and calculations, see, for example, Ref [36], Ch. 4, paragraph 4.5, and Ref. [37]. The occurrence of four contributions to the LT spectrum could also be a signature of an intrinsic property of the $Fe_{1.05}Te$ compound. The unconventional lines intensities ratio of the green subspectrum (Fe2 group, see details in Section 5 (Discussion)) needs further investigation. We expect that ab initio calculation can shed light on this peculiarity [38, 39].

4 *Ab initio* calculations

4.1 Methods

The calculations have been performed by means of density functional theory (DFT) using the Vienna *ab-initio* simulation package (VASP 5.3) [40–43] integrated into MedeA software complex[1]. The electron-ion interactions were described by using the projector-augmented wave (PAW) method. The PAW method is a frozen-core one that uses the exact shape of the valence electrons' wave functions instead of pseudo-wave functions [44]. The Perdew-Burke-Ernzernhof (PBE) generalized gradient approximation (GGA) was used for the exchange and correlation corrections [45]. The Fe ($3d^64s^2$) and Te ($5s^25p^4$) electrons of the valence shell were treated explicitly, whereas remaining electrons of the cores were taken into account by using pseudopotentials. Plane waves (PW) were included into the basis set up to a cutoff of 500 eV. The *k*-point mesh was a $4 \times 4 \times 7$ Monkhorst-Pack grid which corresponds to actual *k*-spacings of $0.137 \times 0.137 \times 0.143$ per Å. Despite the fact that Fe-3*d* electrons are strongly correlated, in Ref. [12] it was argued that density functional theory provides a useful

[1] MedeA version 2.16. MedeA is a registered trademark of Materials Design, Inc., Angel Fire, New Mexico, USA.

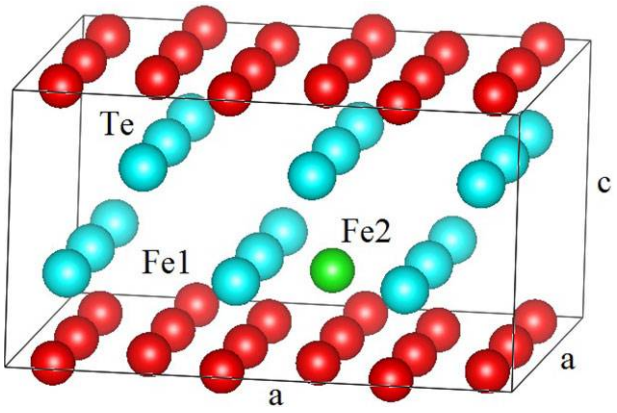

Figure 4 (color online) Structure ($3 \times 3 \times 1$ supercell of FeTe with one excess Fe) used to simulate $Fe_{1.05}Te$ (composition $Fe_{19}Te_{18}$). Iron atoms in the Fe-Te layers are denoted Fe1 (red) and the excess iron as Fe2 (green).

starting point for understanding the electronic properties of iron-chalcogenide materials, and that its description is not improved by inclusion of additional on-site Coulomb terms which is realized in the GGA+U method. So we restricted ourselves to the GGA approach.

Despite of the fact that DFT can calculate the ground state only at $T = 0$ K, in order to simulate the system at room temperature, we used experimental values of the RT lattice parameters and atoms positions [9]. The only parameter that was optimized during the *ab initio* simulations is z-coordinate of the excess iron atom Fe2. The obtained fractional z-coordinate appeared to be 0.717. Electric field gradients at the positions of the atomic nuclei were calculated using the method of Ref. [46].

As was shown in section 2, from Rietveld refinement it follows that the composition of the sample is $Fe_{1.09}Te$ and the occupancy factors of Fe1 and Fe2 atoms are equal to 0.96 and 0.13, respectively. However, the more reliable WDS microanalysis shows that the composition is $Fe_{1.052(4)}Te$. Rietveld refinement shows that the occupancy factor of Fe1 in our sample is close to one. So, we considered our sample as a $Fe_{1.05}Te$ with fully occupied Fe1 site, as usually demonstrated in literature [15, 30–32]. For these reasons we used a $3 \times 3 \times 1$ supercell, which contains 18 Te atoms and 19 Fe atoms including one excess iron atom (Fig. 4). This corresponds to $Fe_{1.055}Te$ with fully occupied Fe1 sites and enables to simulate the experimental sample.

On the other hand, to check that periodic boundary conditions do not influence the EFG tensor of Fe1 atoms, we have increased the size of the supercell up to $4 \times 4 \times 1$. After calculation of the EFG tensors and analyzing their main-axes orientation, we obtained results similar to that for the $3 \times 3 \times 1$ supercell: the main-axes of the EFG tensors of the Fel atoms in the first and second coordination spheres have similar orientation as in the $3 \times 3 \times 1$ supercell, whereas for the rest iron atoms they are oriented like in pure FeTe, *i.e.* their orientation is uncorrelated with the direction to the Fe2 atom.

It is known that $Fe_{1+y}Te$ compounds (y up to 0.08) are paramagnetic at room temperature, and the antiferromagnetic phase transition occurs only at 72.5 K [9, 26]. Indeed, our Mössbauer measurements do not indicate any magnetic order at room temperature. On the other hand, previous *ab initio* calculations demonstrate that the magnetic moment of excess iron atoms in $Fe_{1.125}Te$ is of the order of 2.4 μ_B [12].

So, in order to provide a correct decription of magnetic order in the present $Fe_{1.05}Te$ system, we have performed spin-polarized calculations. The magnetic moment on Fe2 atoms was initialized with a value of 2.5 μ_B, whereas Fe1 atoms initially had no magnetic moments. After calculation of the ground state by means of DFT the Fe2 occupation iron still stayed in the magnetic state $\mu(\text{Fe2}) \approx 2.3\ \mu_B$, whereas the magnetic moments of the Fe1 iron atoms remained almost zero $\mu(\text{Fe1}) \approx 0$.

4.2 *Ab initio* calculations results

Firstly, we consider ideal stoichiometric FeTe which does not contain any excess iron atoms. The crystal structure consists of two formula units of FeTe, *i.e.* there are two iron atoms in an identical environment. The electric field gradient tensor at each atomic position of iron atoms was calculated. The principal axis of the EFG tensor at the iron atoms is parallel to the c-axis of the crystal, whereas the quadrupole splitting (QS) is equal to $QS = -0.152$ mm/s.

Next, the structure with about 5% of excess iron atoms $Fe_{1.055}Te$ was considered. Presence of Fe2 alters the EFG tensors on the nearest Fe1 atoms, *i.e.* values of the quadrupole splitting (QS) and the angle α between the EFG principal axis and the crystallographic c-axis are changed (Fig. 5). Three groups of iron atoms (Fe1/1, Fe1/2 and Fe1) with different EFG parameters can be identified around the excess iron atom Fe2. Two of them with non-zero α form two coordination spheres with radii $R_1 = 1.91$ Å (group Fe1/1) and $R_2 = 4.27$ Å (group Fe1/2), respectively. All more distant (more than 5 Å) iron atoms were attributed to the third group (group Fe1). The obtained results for the EFG parameters are presented in Table 2 (the header "Theory"). It should be noted that the quadrupole splitting referred to the iron atoms in the third group and in the ideal stoichiometric

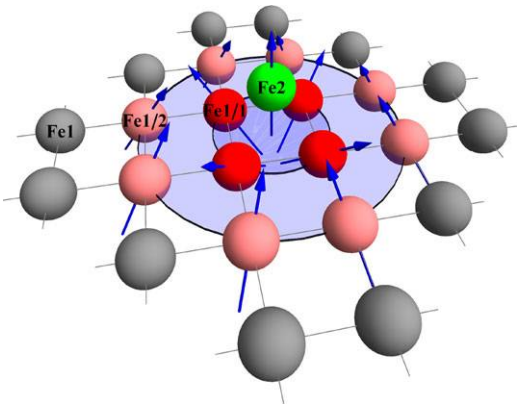

Figure 5 (color online) Schematic representation of the groups of iron atoms within the four-group model. Blue arrows indicate directions of principal axes of EFG tensors.

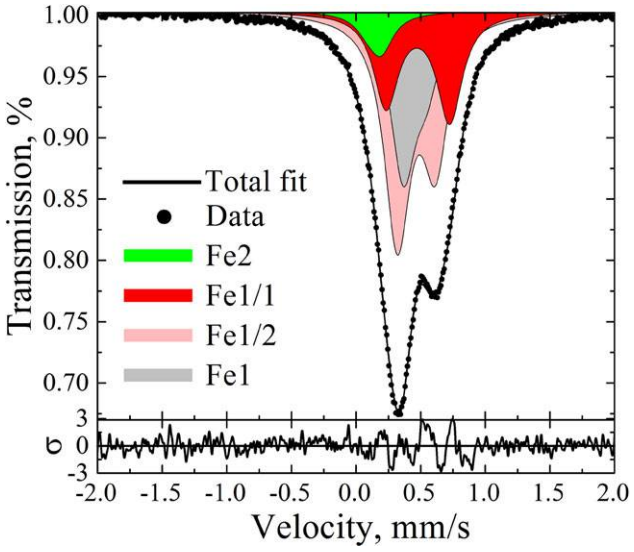

Figure 6 (color online) Room temperature Mössbauer spectrum of single-crystalline $Fe_{1.05}Te$ (black symbols) and subspectra (colored) of the fitting (black line) corresponding to different groups of iron atoms within the four-group model.

Table 2 Parameters for Mössbauer spectra obtained from the *ab inito* calculations and fitting of the Mössbauer experimental data at room temperature.

		Theory			Experiment (RT)			
		α,°	*QS*, mm/s	*W*	α,°	*QS*, mm/s	*W*	*IS*, mm/s
$Fe_{1.05}Te$	Fe2	0	0.178	0.05	0	0.10	0.05	0.14
	Fe1/1	48.89	0.332	0.21	48.5	0.49(2)	0.26	0.47(8)
	Fe1/2	32.46	−0.129	0.42	34.7	−0.29(2)	0.46	0.46(6)
	Fe1	0	−0.163	0.32	0	−0.17(7)	0.23	0.45(5)
FeTe	Fe1	0	−0.152	1.0	—	—	—	—

FeTe are very close to each other (see Table 2, last two lines). Thus, one can deduce that the influence of Fe2 onto iron atoms of the third group is negligible.

Isomer shifts (*IS*) of iron atoms were not calculated in the present work. Nevertheless, we suppose that iron atoms of each group should have their particular value of the isomer shift because of different environment. However, one could assume that these quantities are the same within each iron group and can be obtained from fitting of the experimental data (see Table 2, last column).

Thus, we can conclude that in $Fe_{1.05}Te$ there are four groups of iron atoms which are different by their EFG parameters: three groups of Fe1 iron atoms, and one group of Fe2 iron atoms which contains only excess iron atoms (group Fe2).

5 Discussion

It is known that *ab initio* calculations allow to evaluate electric field gradients only semiquantitatively [46–48]. Nevertheless, the *ab initio* results could the complement analysis of the experimental Mössbauer spectra.

As was shown in the previous section, according to the results of *ab initio* calculations, we have identified four physically distinct groups of iron atoms. Thus, it is reasonable to model RT Mössbauer spectra with four doublets which will be referred as a *four-group model* (Fig. 6). Each of the doublets is characterized by isomer shift (*IS*), quadrupole splitting value (*QS*), angle θ and partial area (*W*). If the *k*-vector is parallel to the *c*-axis of the sample, then θ and α angles are equal. Initial values of *QS* and α for the fitting procedure were taken from *ab initio* calculations (Table 2, under the header "Theory"), whereas the initial value for the isomer shift was taken from Ref. [26] ($IS = 0.45$ mm/s). During the fitting procedure the *IS*, *QS* and α-angle values were changed slightly to better reproduce the experimental spectrum by the proposed model (Fig. 6). The fitted values of *IS*, *QS* and α are presented in Table 2 (columns under the header "Experiment (RT)").

As can be seen from Table 2 the EFG parameters obtained from *ab initio* calculations agree well with the fitted ones: the values of α and *W* are very close; there are some discrepancies for the *QS* values which are rather

expected within DFT approach [46–48], however, the sign of *QS* is always correct.

Individual asymmetry of the partial doublet sub-spectra (most evident for the Fe1/1 (red) and Fe1/2 (pink)) is determined by angles between the electric field gradient (EFG) principle axes (see Fig. 5) and gamma-quanta propagation direction (see Ref. [36], Ch. 4, Table 4.4). The doublet structure of Fe1 and Fe2 sub-spectra are not resolved because of small QS (see in Table 2 under the header "Experiment (RT)") compared to their linewidth, equals to 0.097 mm/s (4.55×10^{-9} eV, natural linewidth, see Ref [36], Ch. 2, paragraph 2.2).

The values of the isomer shift for Fel/1, Fe1/2 and Fe1 iron groups are very close to each other. With increasing the distance from Fe2 excess iron atom they tend to approach 0.452 mm/s, which was reported in Ref. [26]. On the other hand, the *IS* value for the Fe2 group is almost three times smaller. This fact could be explained by various reasons: (i) Fe1 and Fe2 atoms have significantly different local environment and, as a consequence, (ii) the valence states of Fe1 and Fe2 are different. Ref. [12] reported that Fe2 occurs in Fe^{+} valence state whereas Fe1 should have valence 2+. Moreover, the *IS* value for Fe2 obtained in Ref. [26] is also smaller than for Fe1.

In order to confirm the correctness of the refined Mössbauer parameters, the experimental Mössbauer spectrum recorded at the γ-beam incidence angle $\beta = 47^{\circ}$ was compared (Fig. 7) with the simulated spectrum calculated for the same angle and for the same EFG parameters (taken from Table 2, the header "Experiment (RT)"). It could be seen from Fig. 7 that the four-group model is able to describe the angular dependence of the Mössbauer spectra quite well.

Additionally, the correctness of the four-group model is confirmed by the four-sextet modeling of the LT Mössbauer spectrum shown in Fig. 3. The weights of the partial sextets, 0.06, 0.17, 0.46 and 0.31, are very close to the predicted ones from the four-group model (Table 2, third column under the header "Theory"). Each sextet can be attributed to one of the four group of iron: 0.06 (Fe2), 0.17 (Fe1/1), 0.46 (Fe1/2) and 0.31 (Fe1). Moreover, the sextet attributed to the Fe2 group shows a large hyperfine-field value equal to 202.(9) kOe which is characteristic of the magnetic moment on the Fe2 approximately $2\,\mu_B$ [49–51]. It is notable that the sextets attributed to Fe1, Fe1/1 and Fe1/2 groups show line-intensities ratio 3 : 4 : 1 : 1 : 4 : 3. It indicates that the magnetic moments of the iron atoms of the Fe1, Fe1/1 and Fe1/2 groups lie in the sample plane, *i.e.* perpendicular to the *c*-axis of the crystal. Such magnetic ordering for Fe1 iron atoms was reported in numerous papers [13, 14]. Thus, iron atoms in $Fe_{1.05}Te$ are divided into four groups instead of two groups expected from the crystal cell structure.

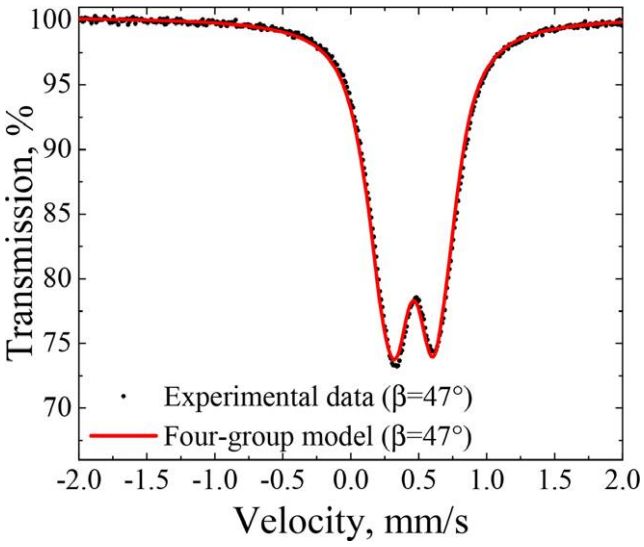

Figure 7 (color online) Experimental room-temperature Mössbauer spectrum of single-crystalline $Fe_{1.05}Te$ obtained for β-angle (between crystallographic *c*-axis of crystal and propagation direction of γ-photons) equal to 47° (black dots) and calculated spectrum by the four-group model for $\beta = 47^{\circ}$ (red line).

In a number of papers [26–29] an asymmetry of Mössbauer spectra of $Fe_{1+y}(Se_{1-x}Te_x)$ powder samples was reported while the spectra are expected to be symmetric doublets. Indeed, FeSe which has crystal structure similar to FeTe, can be prepared as stoichiometric compound [26, 52], *i.e.* without excess iron atoms occupying interlayer 2c (Fe2) positions in the FeSe lattice. Mössbauer spectra of stoichiometric FeSe have shown symmetric doublet despite of the presence of impurity phases like Fe_7Se_8, Fe_3O_4 and α-Fe [52]. In Refs. [27, 29] the asymmetry of the Mössbauer spectra of $FeSe_{1-x}Te_x$ compounds was referred to impurity phases, while in Ref. [26] it was explained by the presence of excess iron atoms in $Fe_{1.08}Te$, however, the influence of Fe2 iron onto Fe1 iron was not considered. In a comparative study of FeSe and $FeSe_{0.5}Te_{0.5}$ powder samples by Mössbauer spectroscopy at temperatures above 70 K [53], it was obtained that the former has a symmetric while the latter has an asymmetric doublet structure. We suppose that it might be a result of an absence of excess iron atoms in FeSe and the presence of them in $FeSe_{0.5}Te_{0.5}$. Our combined Mössbauer experimental and *ab initio* theoretical study of $Fe_{1.05}Te$ single-crystal samples brings evidence that the interlayer iron atoms are the main reason for the observed asymmetry of

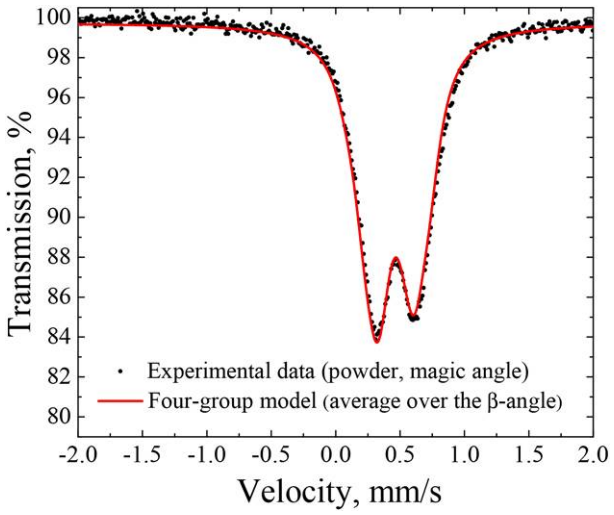

Figure 8 (color online) Experimental room-temperature Mössbauer spectrum of powdered $Fe_{1.05}Te$ sample, recorded at "magic angle" (black line) and simulated spectrum (red line) within the four-group model (average over the β-angle).

doublet in RT Mössbauer spectra. In addition, the four-group model proposed in the present paper explains the asymmetry of Mössbauer spectra of powder samples of $Fe_{1+y}Te$.

Comparison between experimental data, recorded at "magic angle" with respect to the surface normal [54] and simulated (average over the β-angle) powder spectrum within the four-group model is presented in Fig. 8. As far as each of the groups Fe1, Fe1/1 and Fe1/2 have peculiar angle between the EFG principle axis and the crystallographic axes of the crystal, there is no common "magic angle" for all magnetic centers of the sample. The spectrum keeps a shape of asymmetric doublet. Small disagreement could be a result of preferred orientation of the crystallites (texture), which is actually observed in our XRD measurements. Moreover, the fraction of Fe2 atoms could increase during powder sample preparation, whereas in the present case this parameter is fixed. The *ab inito* calculations allowed us to conclude that excess iron atoms Fe2 can significantly affect the charge density in the $Fe_{1+y}Te$ compounds up to the second coordination sphere.

6 Conclusion

The results of the present study demonstrate that Mössbauer spectra of iron in $Fe_{1.05}Te$ can be well described by a model of four non-equivalent groups of iron atoms. Three of them are located within the Fe-Te layers, while the fourth group consists of excess iron atoms. The model is confirmed by *ab inito* calculations which show good agreement of the calculated parameters of the Mössbauer spectra with those derived from the fitting of the experimental spectra acquired at room and low temperatures. The angular dependence of the spectra is also well described by this model. We conclude that non-stoichiometric iron atoms Fe2 affect the charge-density distribution up to the second coordination sphere of irons. The Mössbauer measurements at low temperatures indicate that the spin density is perturbed as well. It should complicate magnetic order which has already been reported [13, 14]. It is worthy to note that even a small amount of excess iron atoms leads to modification of the electronic properties of the Fe-Te layers in $Fe_{1.05}Te$. Moreover, we have shown that differentiation of the iron atoms into four groups is a reason for the asymmetry of the Mössbauer spectra for powdered samples of $Fe(Se_{1-x}Te_x)$ compounds, reported in previous papers [26–29]. We presume that our results could be extended on the entire class of $Fe_{1+y}Se_{1-x}Te_x$ compounds which contain excess iron atoms.

Acknowledgements. The authors thank Dr. H.-A. Krug von Nidda for discussion and valuable comments on the manuscript. The authors from KFU acknowledge partial support by the Ministry of Education and Science of the Russian Federation within the subsidy allocated to Kazan Federal University and the Program of Competitive Growth of Kazan Federal University (F.G.V. and L.R.T.). A. G. Kiiamov received financial support from German Academic Exchange Servise (DAAD). This work was partially supported by the German Research Foundation (DFG) within the Transregional Collaboration Research Centre TRR80 "From Electronic Correlation to Functionality" (Augsburg, Munich, Stuttgart). The Mössbauer measurements and partially XRD measurements were carried out at the PCR Federal Center of Shared Facilities of KFU.

Key words. iron chalcogenides, mössbauer spectroscopy, *ab initio*.

References

[1] Y. Kamihara, T. Watanabe, M. Hirano, and H. Hosono, J. Am. Chem. Soc. **130**(11), 3296–3297 (2008).
[2] J. Paglione and R. L. Greene, Nat. Phys. **6**, 645–658 (2010).
[3] G. R. Stewart, Rev. Mod. Phys. **83**(4), 1589 (2011).
[4] X. Chen, P. Dai, D. Feng et al., Nat. Sci. Rev. **1**, 371–395 (2014).
[5] F. C. Hsu, J. Y. Luo, K. W. Yeh et al., Proc. Nat. Acad. Sci. **105**(38), 14262–14264 (2008).

[6] Y. Mizuguchi, F. Tomioka, S. Tsuda et al., Appl. Phys. Lett. **93**(15) (2008).
[7] S. Medvedev, T. McQueen, I. Troyan et al., Nat. Mater. **8**(8), 630–633 (2009).
[8] M. Fang, H. Pham, B. Qian et al., Phys. Rev. B **78**(22), 224503 (2008).
[9] A. Martinelli, A. Palenzona, M. Tropeano et al., Phys. Rev. B **81**(9), 094115 (2010).
[10] F. Gronvold, H. Haraldsen, and J. Vihovde, Acta Chemica Scand. **8**(10), 1927–1942 (1954).
[11] D. Finlayson, D. Greig, J. Llewellyn, and T. Smith, Proc. Phys. Soc. Sec. B **69**(8), 860 (1956).
[12] L. Zhang, D. J. Singh, and M. H. Du, Phys. Rev. B **79**(1), 012506 (2009).
[13] E. E. Rodriguez, C. Stock, P. Zajdel et al., Phys. Rev. B **84**(6), 064403 (2011).
[14] M. Enayat, Z. Sun, U. R. Singh et al., Science **345**(6197), 653–656 (2014).
[15] R. Viennois, E. Giannini, D. VanDer Marel, and R. Černỳ, J. Solid State Chem. **183**(4), 769–775 (2010).
[16] S. Cao, S. Shen, L. Chen et al., J. Appl. Phys. **110**(3), 033914 (2011).
[17] G. Chen, Z. Chen, J. Dong et al., Phys. Rev. B **79**(14), 140509 (2009).
[18] M. Z. Cieplak and V. Bezusyy, Phil. Mag. **95**(5-6), 480–492 (2015).
[19] J. Li, G. Huang, and X. Zhu, Physica C: Supercond. **492**, 152–157 (2013).
[20] M. J. Han, Q. Yin, W. E. Pickett, and S. Y. Savrasov, Phys. Rev. Lett. **102**(10), 107003 (2009).
[21] H. Shi, Z. B. Huang, S. T. John, and H. Q. Lin, J. Appl. Phys. **110**(4), 043917 (2011).
[22] M. Monni, F. Bernardini, G. Profeta, and S. Massidda, Phys. Rev. B **87**(9), 094516 (2013).
[23] F. Ma, W. Ji, J. Hu et al., Phys. Rev. Lett. **102**(17), 177003 (2009).
[24] T. Miyake, K. Nakamura, R. Arita, and M. Imada, J Phys. Soc. Jap. **79**(4), 044705 (2010).
[25] T. McQueen, Q. Huang, V. Ksenofontov et al., Phys. Rev. B **79**(1), 014522 (2009).
[26] Y. Mizuguchi, T. Furubayashi, K. Deguchi et al., Physica C: Supercond. **470**, S338–S339 (2010).
[27] R. Gómez, V. Marquina, J. Pérez-Mazariego et al., J. Supercond. Nov. Magn. **23**(4), 551–557 (2010).
[28] K. Reddy and S. Chetty, Phys. Stat. Solidi (a) **37**(2), 687–694 (1976).
[29] K. Szymański, W. Olszewski, L. Dobrzyński et al., Supercond. Sci. Techn. **24**(10), 105010 (2011).
[30] C. Koz, S. Rößler, A. Tsirlin et al., Phys. Rev. B **86**(9), 094505 (2012).
[31] D. Louca, K. Horigane, A. Llobet et al., Phys. Rev. B **81**(13), 134524 (2010).
[32] S. Li, C. de La Cruz, Q. Huang et al., Phys. Rev. B **79**(5), 054503 (2009).
[33] J. Lindén, J. P. Libäck, M. Karppinen et al., Solid State Commun. **151**(2), 130–134 (2011).
[34] S. Margulies and J. Ehrman, Nucl. Instrum. Meth. **12**, 131–137 (1961).
[35] V. Goldanskii, E. Makarov, and V. Khrapov, Phys. Lett. **3**(7), 344–346 (1963).
[36] P. Gütlich, E. Bill, and A. X. Trautwein, Mössbauer spectroscopy and transition metal chemistry: fundamentals and applications (Springer Science & Business Media, 2010), 568 p.
[37] D. Satuła, K. Szymański, L. Dobrzyński, V. Tran, and R. Troć, Phys. Rev. B **78**(1), 014411 (2008).
[38] A. Błachowski and U. Wdowik, Acta Phys. Pol. A **119**(1), 24–27 (2011).
[39] A. Błachowski and U. D. Wdowik, J. Phys. Chem. Solids **73**(2), 317–323 (2012).
[40] G. Kresse and J. Hafner, Phys. Rev. B **47**, 558 (1993).
[41] G. Kresse and J. Hafner, Phys. Rev. B **49**, 14251–14269 (1994).
[42] G. Kresse and J. Furthmuller, Comp. Mater. Sci. **6**, 15–50 (1996).
[43] G. Kresse and J. Furthmuller, Phys. Rev. B **54**, 11169–11186 (1996).
[44] P. E. Blöchl, Phys. Rev. B **50**(24), 17953 (1994).
[45] J. P. Perdew, K. Burke, and M. Ernzerhof, Phys. Rev. Lett. **77**(18), 3865 (1996).
[46] H. M. Petrilli, P. E. Blöchl, P. Blaha, and K. Schwarz, Phys. Rev. B **57**(23), 14690 (1998).
[47] P. Schwerdtfeger, T. Söhnel, M. Pernpointner et al., J. Chem. Phys. **115**(13), 5913–5924 (2001).
[48] I. Kantor, L. Dubrovinsky, C. McCammon et al., Phys. Rev. B **80**(1), 014204 (2009).
[49] D. Welz, P. Deppe, W. Schaefer, H. Sabrowsky, and M. Rosenberg, J. Phys. Chem. Solids **50**(3), 297–308 (1989).
[50] M. Nishi, Y. Ito, and A. Ito, J. Phys. Soc. of Jpn. **52**(10), 3602–3610 (1983).
[51] H. P. Nissen and K. Nagorny, Z. Phys. Chem. Neue Folge **99**(4-6), 209–216 (1976).
[52] A. Błachowski, K. Ruebenbauer, J. Żukrowski et al., J. Alloy. Comp. **494**(1), 1–4 (2010).
[53] S. I. Shylin, V. Ksenofontov, S. A. Medvedev, and C. Felser, J. Supercond. Nov. Magn. **29**(3), 573–576 (2015).
[54] J. Greneche and F. Varret, Journal de Physique Lettres **43**(7), 233–237 (1982).